Tellus (1993), 45A, 325–340
Printed in Belgium – all rights reserved

TELLUS
ISSN 0280–6495

Residual currents in tidally dominated, well-mixed estuaries

By ROBERT K. McCARTHY, *College of Marine Studies, University of Delaware, Newark, DE 19716, USA*

(Manuscript received 6 July 1992; in final form 6 April 1993)

ABSTRACT

An analytical model is developed to investigate the residual circulation originating from the interaction of the density field, river flow, and the nonlinear rectification of the periodic tides, in tidally-dominated, well-mixed estuaries. These residual flows effect the density field, which in turn drives the estuarine gravitational circulation. Previous analytical studies have excluded the tidal dynamics and have either imposed the density structure, thereby decoupling the problem, or assumed similarity solutions valid for specific regions within the estuary. Here, a theoretical model is developed that calculates, via a perturbation analysis, the lowest-order density field established from tidal mixing, tidally-induced residual flow, river runoff, and diffusion. Two special cases are considered, a long tidal river and a finite length, variable-breadth estuary. Once the density field is determined for each case, the density driven flow is calculated and added to the rectified tidal and river induced flows for both the Eulerian and Lagrangian reference frames.

1. Introduction

This work describes the tidal and residual circulation in tidally dominated, well mixed estuaries. Here the phrase "tidally dominated" means that, on average, the barotropic tidal motion contains the bulk of the energy. Although the instantaneous flow is dominated by barotropic tidal currents, the transport and dispersion of salt, pollutants, larvae and other waterborne materials depend primarily on low-frequency and mean motions. These low-frequency, or residual, flows result primarily from the interaction of the density field, river flow, and the nonlinear rectification of the periodic tides, and typically have time scales on the order of 2 weeks or more. Wind forcing can also produce low-frequency flows, but will be ignored here.

Oceanographers have known for decades that the residual circulation in estuaries caused by the density difference between fresh and ocean water consists of the surface layers flowing seaward and the bottom layers flowing landward. Previous analytical studies of this two-layer circulation include Rattray and Hansen (1962), Hansen and Rattray (1965, 1966), Hansen (1967), Officer (1976), Chatwin (1976), and Oey (1984). These studies were guided by Pritchard's (1952, 1954, 1956) quantitative analysis of the conservation of salt equation in which he determined that longitudinal advection balances vertical diffusion. Accordingly, they neglected the rectified tidal flow and its coupling to the density field. Hansen and Rattray (1965) found similarity solutions to the density field for the central and inner regimes, thereby avoiding the need to specify the density structure a priori to calculate the density driven flow.

An important contribution to the coupled problem of estuarine circulation was provided by Jay (1987) and Jay and Smith (1990a, 1990b). Their model, which was motivated by observations of the Columbia River estuary, incorporated the interaction of the barotropic tides (Ianniello 1977a) with the baroclinic forcing established from the horizontal density gradient. For weak stratification, where the vertical density difference is much smaller than the horizontal density difference, they found from a two-parameter expansion technique that the residual flow consisted of the sum of the nonlinearly induced residual flow and the density driven flow. However, they also assumed that the mean horizontal density gradient

was spatially and temporally constant and they omitted horizontal diffusion. Therefore, their major balance was between tidal advection of the imposed uniform density field and vertical diffusion.

Here, we determine the density field through an internally consistent perturbation scheme, and then use this density field to compute the steady state, density-driven flow. Hence, the density field is coupled to the circulation, as in nature, and the effects of tidal mixing and tidally induced residual flow, including its interaction with the river, are explicitly included.

The model formulation, scalings, and expansions are discussed in Section 2. Once the scaled equations are reduced to lowest order, the solution to the density field is calculated for an infinitely long, constant breadth and depth estuary in Section 3. Complete mixing occurs within the estuary by assuming the ocean is a constant density reservoir. Residual flows are then calculated. A finite-length, variable-breadth estuary geometry is considered in Section 4, and Section 5 summarizes the model results.

2. The model

The model will be restricted to a tidally dominated, well-mixed estuary with the fresh water entering from the head only. The well-mixed constraint limits the model to an estuary whose vertical density change, $\Delta_v \rho$, is small compared to the longitudinal density variation, $\Delta_h \rho$. Excluded from the discussion will be partially mixed and salt wedge estuaries.

The present model includes the baroclinic pressure gradient term resulting from horizontal density differences within the estuary, and hence there is the need for an additional density equation to close the problem. A similar perturbation technique to Ianniello's (1977a, 1977b, 1979, 1981) is followed. The novel features of the model are that the density and the density driven flow in the channel are coupled to the complete circulation, and the effects of tidal mixing and the nonlinearly induced residual currents are explicitly included. The inherently nonlinear problem is made mathematically linear by a physical constraint on the density field.

Most of the model assumptions are those used by Ianniello (1977a) to reduce the 3-dimensional problem to a 2-dimensional, horizontal and vertical (x, z), problem. The estuary will have rectangular cross section and constant depth, while the breadth will vary exponentially to model the shape of many estuaries. The coordinate system is shown in Fig. 1, where x is positive longitudinally away from the mouth toward the head, and z is positive up with the bottom at $z = -h$.

The governing dimensional longitudinal momentum, breadth integrated continuity, and depth and breadth integrated continuity equations are

$$\frac{\partial u}{\partial t} + u\frac{\partial u}{\partial x} + w\frac{\partial u}{\partial z} = -g\frac{\partial \eta}{\partial x} - \frac{g}{\rho_c}\int_z^\eta \frac{\partial \rho}{\partial x}\,dz + N_z\frac{\partial^2 u}{\partial z^2}, \tag{1}$$

$$\frac{\partial u}{\partial x} + \frac{\partial w}{\partial z} = -u\frac{b'(x)}{b(x)}, \tag{2}$$

$$\frac{\partial}{\partial x}\left(b\int_{-h}^{0} u\,dz\right) + \frac{\partial}{\partial x}\left(b(u|_{z=0}\,\eta)\right) + b\frac{\partial \eta}{\partial t} = 0, \tag{3}$$

where u is the longitudinal velocity component, w is the vertical velocity component, η is the free surface elevation above $z = 0$, ρ is the density, ρ_c is a mean density, g is the acceleration of gravity, b is the breadth, h is the depth, and N_z is the vertical

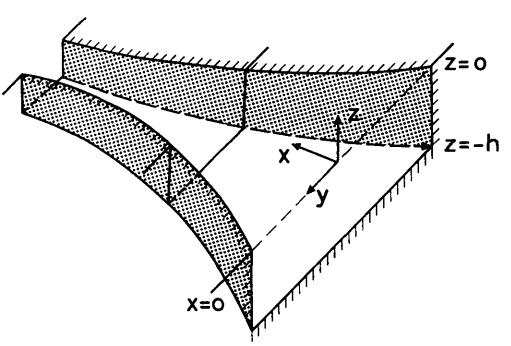

Fig. 1. Model geometry. The coordinate axes are located at the mouth of the channel, with positive longitudinal distance to the left. The depth is constant and the breadth is allowed exponential decay away from the mouth.

eddy viscosity coefficient, here assumed constant. (Ianniello has demonstrated that use of constant vertical eddy viscosity reproduces all the important features of both the tidal solution and the nonlinearly induced flow.)

The above equations are the same as those used by Ianniello (1977a), apart from the addition of the baroclinic pressure gradient term in eq. (1), resulting from the longitudinal density difference within the estuary. Since this new forcing term is unknown, a density equation is required to close the problem. The following equation represents the balance of density advection and diffusion in the estuary.

$$\frac{\partial \rho}{\partial t} + u\frac{\partial \rho}{\partial x} + w\frac{\partial \rho}{\partial z} = K_x\frac{\partial^2 \rho}{\partial x^2} + K_z\frac{\partial^2 \rho}{\partial z^2}. \tag{4}$$

Here both the longitudinal and vertical eddy diffusivities, K_x and K_z, are assumed constant, and lateral advection and diffusion have been neglected, since the density field is assumed laterally homogeneous.

In order to simplify the problem, a scaling analysis of the governing equations is useful. Following Ianniello (1977b), we introduce the scaling as

$$t = (1/\sigma)\,\hat{t},$$

$$\eta = \eta_m \hat{\eta},$$

$$x = \frac{c}{\sigma}\hat{x},$$

$$h = (2N_z/\sigma)^{1/2}\,\hat{d},$$

$$z = (2N_z/\sigma)^{1/2}\,\hat{z},$$

$$b(x) = b_m \hat{b}(x),$$

$$u = \frac{\eta_m}{h} c\hat{u},$$

$$w = (2N_z\sigma)^{1/2}\frac{\eta_m}{h}\hat{w},$$

where a caret (^) denotes a scaled quantity. Here, σ is the angular frequency of tidal forcing, η_m is the sea level amplitude at the mouth, b_m is the breadth at the mouth, c is the shallow water wave phase speed, and $(2N_z/\sigma)^{1/2}$ is the frictional depth scale.

The estuary will be modeled as a mixing zone between two reservoirs of uniform density that differ by $\Delta_h\rho$, a known amount. The density will be written in terms of a constant density of freshwater plus a longitudinal density difference. The density difference, in turn, is scaled by $\Delta_h\rho$. Mathematically, $\rho = \rho_{fresh} + \Delta_h\rho\hat{\rho}$, where $\hat{\rho}$ is the scaled density difference. When $\hat{\rho} = 1$, the density is that of ocean water, while when $\hat{\rho} = 0$, the density is that of freshwater.

A useful choice for the scaling for the horizontal eddy diffusivity is

$$K_x = \varepsilon^2 c^2/\sigma\hat{K}_x,$$

where $\varepsilon \equiv \eta_m/h \ll 1$, a measure of the nonlinearity of the system. This will be shown later in Section 3 to result from a balance between downstream advection of buoyancy by the Lagrangian subtidal flow and upstream transport by diffusion.

Substituting the scaled variables into eqs. (1), (3), and (4), gives

$$\frac{\partial \hat{u}}{\partial \hat{t}} + \varepsilon\left(\hat{u}\frac{\partial \hat{u}}{\partial \hat{x}} + \hat{w}\frac{\partial \hat{u}}{\partial \hat{z}}\right) = -\frac{\partial \hat{\eta}}{\partial \hat{x}} - \varepsilon\gamma\int_{\hat{z}}^{0}\frac{\partial \hat{\rho}}{\partial \hat{x}}\,d\hat{z} - \varepsilon^2\gamma\hat{\eta}\hat{d}\frac{\partial \hat{\rho}}{\partial \hat{x}} + \frac{1}{2}\frac{\partial^2 \hat{u}}{\partial \hat{z}^2}, \tag{5}$$

$$\frac{1}{\hat{d}}\frac{\partial}{\partial \hat{x}}\left(\hat{b}\int_{-\hat{d}}^{0}\hat{u}\,d\hat{z}\right) + \varepsilon\frac{\partial}{\partial \hat{x}}\left(\hat{b}(\hat{u}|_{z=0}\,\hat{\eta})\right) + \hat{b}\frac{\partial \hat{\eta}}{\partial \hat{t}} = 0, \tag{6}$$

$$\frac{\partial \hat{\rho}}{\partial \hat{t}} + \varepsilon\left(\hat{u}\frac{\partial \hat{\rho}}{\partial \hat{x}} + \hat{w}\frac{\partial \hat{\rho}}{\partial \hat{z}}\right) = \varepsilon^2\hat{K}_x\frac{\partial^2 \hat{\rho}}{\partial \hat{x}^2} + \frac{1}{2}\hat{S}_c\frac{\partial^2 \hat{\rho}}{\partial \hat{z}^2}, \tag{7}$$

where $\gamma \equiv \Delta_h\rho/(\rho_c\varepsilon^2 d)$, and $\hat{S}_c = K_z/N_z$ is the Schmidt number. Note that ε also scales the advection of density in eq. (7), as was previously shown by Feng et al. (1986). Since $\varepsilon \ll 1$, the nonlinear advection terms do not effect the tidal solution. Therefore, ε will be the expansion parameter for the dependent variables. Thus the model is restricted to weakly nonlinear estuaries.

$\varepsilon\gamma$ measures the strength of the baroclinic forcing term in eq. (5). Three possibilities arise as to the order of $\varepsilon\gamma$: $\varepsilon\gamma \geqslant O(1)$, $\varepsilon\gamma < O(\varepsilon)$, or $\varepsilon\gamma = O(\varepsilon)$.

If $\varepsilon\gamma \geqslant O(1)$, then the baroclinic forcing term will be as large as or larger than the tidal acceleration term. Then the estuary will no longer be dominated by barotropic tides, in contrast to the model assumption, since the baroclinic pressure gradient will drive an O(1) baroclinic tide. Jay (1987) and Jay and Smith (1990a) showed that when there exists an O(1) baroclinic tide, stratification will also be O(1). If $\varepsilon\gamma < O(\varepsilon)$, or equivalently $\gamma < O(1)$, then the density driven flow is much weaker than the rectified tidal flow. For flows to $O(\varepsilon)$, the fluid can then be considered homogeneous, thus returning to the work of Ianniello. However, for $\varepsilon\gamma = O(\varepsilon)$, or equivalently $\gamma = O(1)$, the relative strengths of the barotropic and baroclinic forcing terms for the residual flows will be comparable. Jay (1987) and Jay and Smith (1990b) showed that, for this case, stratification will be weak, due to the lack of a strong gravitational restoring force. The case when $\gamma = O(1)$ is that of interest here. However, the case $\gamma < O(1)$ can be trivially included by taking small values of γ.

The scaling for K_x results in the horizontal diffusion term being of $O(\varepsilon^2)$ in eq. (7). Thus, horizontal diffusion can be neglected through order ε, but will be important at higher orders.

Since γ is now restricted to be less than or equal order unity, the dependent variables u, η, and w are now expanded in an asymptotic series only in powers of ε,

$$\hat{u} = \hat{u}_1 + \varepsilon\hat{u}_2 + \cdots,$$

$$\hat{\eta} = \hat{\eta}_1 + \varepsilon\hat{\eta}_2 + \cdots,$$

$$\hat{w} = \hat{w}_1 + \varepsilon\hat{w}_2 + \cdots,$$

where $(\,)_1$ represents a term at the fundamental tidal time scale and $(\,)_2$ indicates a steady state and double frequency correction to the tidal solution.

The scaled density field, $\hat{\rho}$, is also expanded in an asymptotic series in powers of ε,

$$\hat{\rho} = \hat{\rho}_0(x, z, t) + \varepsilon\hat{\rho}_1(x, z, t) + \cdots,$$

where $\hat{\rho}_0$ indicates a steady state background density field (as will be shown below), and $\hat{\rho}_1$ also represents a term at the tidal time scale.

The above expansions are inserted into the scaled governing equations, and terms of equal powers of ε are equated. The O(1) or lowest order momentum and continuity equations are identical to those of Ianniello, and hence omitted here. The lowest order density equation is

$$\frac{\partial\rho_0}{\partial t} = \frac{1}{2} S_c \frac{\partial^2\rho_0}{\partial z^2}, \tag{8}$$

where the carets have been omitted. (Henceforth, all variables will be nondimensional unless otherwise noted.)

Eq. (8) states that temporal changes in the background density ρ_0 are produced only by vertical diffusion. But since the boundary conditions at the free surface and bottom stipulate zero buoyancy flux, this time dependence is spurious. Vertical integration of eq. (8) over the whole depth shows that the time derivative of the vertical integral of ρ_0 must vanish. Thus, if $\partial\rho_0/\partial t$ were zero initially everywhere, it would remain so. This steady state character of the background density field is appropriate for a well mixed estuary. Consistent with this property, eq. (8) then gives $\partial^2\rho_0/\partial z^2 = 0$, but since $\partial\rho_0/\partial z = 0$ at both surface and bottom, we have $\partial\rho_0/\partial z = 0$ everywhere. Thus we deduce the important simplification: $\rho_0 = \rho_0(x)$ only, implying that the estuary is well mixed to lowest order. Therefore, tidally dominated estuaries have weak stratification.

The $O(\varepsilon)$ or second order terms contain both a zero and double frequency term (Ianniello 1977a). Thus the advection terms, $u_1\,\partial u_1/\partial x$ and $w_1\,\partial u_1/\partial z$, which are each the product of two terms at the fundamental tidal frequency σ, are the forcing for the nonlinearly induced flow, and thus generate both a double frequency (2σ) and a steady-state component. The steady state terms force the residual flow that is of interest here. Thus, the second order terms will be time averaged, denoted by an overbar, thereby filtering out the double frequency terms from the model. The residual or $O(\varepsilon)$ x-momentum equation, now with $\rho_0 = \rho_0(x)$ only, is

$$\overline{u_1\frac{\partial u_1}{\partial x}} + \overline{w_1\frac{\partial u_1}{\partial z}} = -\overline{\frac{\partial\eta_2}{\partial x}} + \gamma z\frac{\mathrm{d}\rho_0}{\mathrm{d}x} + \frac{3}{8}\frac{\partial^2\overline{u_2}}{\partial z^2}. \tag{9}$$

This equation represents a balance between the advection of the tidal momentum, a barotropic pressure gradient force, a baroclinic pressure gradient force, and vertical friction. (Ianniello (1977a) has shown that the stress representation is

reduced by a factor of 3/4 for the O(ε) terms. There is also a 1/2 factor from the scaling; hence the 3/8 factor in the frictional term in eq. (9).)

The x-integrated O(ε) continuity equation is

$$b(x)\frac{1}{d}\int_{-d}^{0}\overline{u_2}\,dz + b(x)\,\overline{u_1|_{z=0}\,\eta_1} = -R, \qquad (10)$$

where $-R$ is the constant of integration. The first term is just the depth averaged Eulerian current. Longuet-Higgins (1969) showed that the second term, $\overline{u_1|_{z=0}\,\eta_1}$, is equal to the depth integrated Stokes velocity. Thus eq. (10) shows that the depth integrated residual Eulerian flow plus the depth integrated Stokes drift equals $-R$, the net Lagrangian flow through the estuary; here equal to the scaled river flow. We restrict all fresh water to enter at the estuary head, so R is indeed a constant.

R is the ratio of the dimensional river flow $u_r = V_L/b_m h$ to the scale for the nonlinear flow $u_{n1} = \varepsilon^2 c$. Thus $R \equiv u_r/u_{n1} = V_L h/b_m \eta_m^2 c$, where V_L is the volume flux of fresh water entering from the head only. R is equal to the nondimensional parameter $P \equiv u_r/u_t$ used by Hansen and Rattray (1966), divided by ε. Thus, $R = P/\varepsilon$. From the above O(ε) continuity eq. (10), R cannot exceed order one. Therefore $R \leqslant O(1)$, implying that $P \leqslant O(\varepsilon)$. This is consistent with the well mixed case of Hansen and Rattray: $P \ll 1$.

The O(ε) density equation, now with $\rho_0 = \rho_0(x)$ only, is

$$\frac{\partial \rho_1}{\partial t} + u_1\frac{d\rho_0}{dx} = \frac{1}{2}S_c\frac{\partial^2 \rho_1}{\partial z^2}. \qquad (11)$$

This balance at the tidal frequency is between the local rate of change of the first order correction to the background density field, the tidal advection of this background density field, and vertical mixing.

In order to find the density driven flow, the solution for $\rho_0(x)$ is needed to evaluate the baroclinic drive term in eq. (9). Since eq. (11) contains two unknowns, ρ_0 and ρ_1, another equation is needed that relates ρ_0 to ρ_1. Since $\rho_0 = \rho_0(x)$ only, the required condition is a time averaged, vertically integrated form of the density equation which will remove the independent variables t and z, while retaining x. The procedure is fully discussed in McCarthy (1991), hereafter referred to as M91, and only outlined here. The dimensional density equation (4) is vertically integrated using the boundary conditions of no buoyancy flux through the surface and bottom. The remaining terms are rewritten using Leibniz' theorem for differentiating an integral. Simplification occurs using the dimensional free surface boundary condition and continuity. Next the integrals are expanded in Taylor series about $z = 0$, and the resulting governing equation scaled. The scaled, depth integrated density equation is time averaged over time T long compared to a tidal period. Expanding the dependent variables in terms of ε gives the order ε equation,

$$\frac{d}{dx}\left(b(x)\int_{-d}^{0}(\overline{u_1\rho_0})\,dz\right) = 0, \qquad (12)$$

which is equivalent to a time averaged and depth integrated form of eq. (11), and the order ε^2 equation,

$$\begin{aligned} &d^{-1}\frac{d}{dx}\left(b(x)\int_{-d}^{0}\overline{u_1\rho_1}\,dz\right) \\ &+ d^{-1}\frac{d}{dx}\left(b(x)\int_{-d}^{0}\overline{u_2\rho_0}\,dz\right) \\ &+ \frac{d}{dx}\left(b(x)(\overline{u_1\rho_0)|_{z=0}\,\eta_1}\right) \\ &- b(x)\,K_x\frac{d^2\rho_0}{dx^2} = 0, \end{aligned} \qquad (13)$$

where now K_x is introduced.

Because $\partial\rho_0/\partial t = 0$, eq. (12) is satisfied identically, since $\overline{u_1} = 0$. Instead, eq. (13) provides the needed constraint on ρ_0.

The appearance of the product $\overline{u_2\rho_0}$ in eq. (13), representing the advection of the background density field by the residual Eulerian velocity, illustrates the formal nonlinearity in the order ε^2 problem. This is to be expected, because the density driven flow will produce advection of the density field itself. However, the nonlinearity is only formal. Notice that, since ρ_0 is only a function of x, ρ_0 can be factored from the second and third terms. These terms now combine using the continuity eq. (10) to give $d(-R\rho_0)/dx$. Thus it is the known Lagrangian flow that advects the background density field. Since all the fresh water

enters from the head only, $R \neq R(x)$; thus eq. (13) can be rewritten as the linear equation

$$d^{-1}\frac{\mathrm{d}}{\mathrm{d}x}\left(b(x)\int_{-d}^{0}\overline{u_1\rho_1}\,\mathrm{d}z\right)-R\frac{\mathrm{d}\rho_0}{\mathrm{d}x}$$

$$-b(x)\,K_x\frac{\mathrm{d}^2\rho_0}{\mathrm{d}x^2}=0. \qquad (14)$$

Notice what has been accomplished. The nonlinear equation (13) has been reduced, with the help of the depth integrated continuity equation, to the linear equation (14) because of the well mixed constraint on the density field. Had ρ_0 instead been a function of z, the nonlinear term $\overline{u_2\rho_0}$ could not have been factored. Eq. (14) governs ρ_0 and represents a balance between tidal buoyancy transport, Lagrangian subtidal buoyancy transport, and diffusive buoyancy transport. This equation, which also contains the unknowns ρ_0 and ρ_1, can be solved together with eq. (11) to evaluate ρ_0 which will then determine the density driven flow.

3. The long tidal river solution

In this section, we find analytical solutions to the lowest order density field and resulting gravitational circulation for an infinite length estuary of constant depth and breadth. Therefore, in this section, $b(x)=1$. This geometry is suggestive of a long tidal river. The fresh water enters from the head only, and the tidal properties are imposed at the mouth.

The O(1) tidal solutions of Ianniello (1977b) apply here, with

$$\eta_1=\mathrm{Re}(A(x)\,\mathrm{e}^{it}), \qquad (15)$$

$$u_1=\mathrm{Re}(iA'(x)\,U(z)\,\mathrm{e}^{it}). \qquad (16)$$

Here, Re indicates the real part of the solution, $i=(-1)^{1/2}$ and the prime ($'$) indicates a derivative with respect to the independent variable x. At the bottom, a no-slip boundary condition is imposed and at the surface, a no shear stress condition is specified. See Ianniello (1977b) and M91 for solution techniques and the functional forms for $A(x)$ and $U(z)$, and for the solution to w_1 found from integrating eq. (2). By specifying d, the water depth scaled by the frictional depth, the dimensionless first order tidal solution, u_1, η_1, and w_1, can be calculated for estuaries with constant depth, breadth, and N_z.

The nondimensional eqs. (9) and (10) represent the time averaged O(ε) x-momentum and continuity equations. In addition to the rectified tidal flow studied by Ianniello, two other sources of residual flow, the river induced flow, $\overline{u_{2\mathrm{r}}}$, and the density driven flow, $\overline{u_{2\mathrm{d}}}$, contribute to the second order flow. Because the mathematical problem is linear, we can write:

$$\overline{u_2}=\overline{u_{2\mathrm{nl}}}+\overline{u_{2\mathrm{r}}}+\overline{u_{2\mathrm{d}}},$$

$$\overline{\eta_2}=\overline{\eta_{2\mathrm{nl}}}+\overline{\eta_{2\mathrm{r}}}+\overline{\eta_{2\mathrm{d}}}.$$

The no slip boundary condition ($\overline{u_2}|_{-d}=0$) is applied to each flow separately, since these flows are linearly independent. The no-shear condition at the surface is now, see Ianniello (1981),

$$\left.\frac{\partial\overline{u_{2\mathrm{nl}}}}{\partial z}\right|_0=-\mathrm{d}\overline{\eta_1\left.\frac{\partial^2u_1}{\partial z^2}\right|_0}$$

and

$$\left.\frac{\partial\overline{u_{2\mathrm{r}}}}{\partial z}\right|_0=\left.\frac{\partial\overline{u_{2\mathrm{d}}}}{\partial z}\right|_0=0.$$

Thus, eqs. (9) and (10) can be simply rewritten as 3 separate pairs of equations, corresponding to the rectified tidal flow (studied by Ianniello (1977b)), the river induced flow, and the density driven flow. Ianniello (1977b) showed that the depth integrated, nonlinearly induced Lagrangian mean flow, $\overline{u_{2\mathrm{l}}}$ as given in M91, must equal zero (Longuet-Higgins, 1969). The river contribution ($-R$) now only appears in the continuity equation for the river induced flow. Since the river flow and the density driven flow are time independent, the Lagrangian mean velocity equals the Eulerian mean velocity.

The solution to $\overline{u_{2\mathrm{nl}}}$, the rectified tidal flow, appears in M91 with the 3/4 shear stress reduction, but is omitted here. The solution to the river induced flow is easily shown to be

$$\overline{u_{2\mathrm{r}}}(z)=\tfrac{3}{2}R/d^2(z^2-d^2). \qquad (17)$$

Thus the river flow distribution is parabolic with depth and independent of along estuary position for constant breadth estuaries. This distribution

is generally found for open channel flows with constant N_z.

The momentum equation for the density driven flow is similar to the momentum equation for the river induced flow, except for the additional forcing term, $\gamma z\, \mathrm{d}\rho_0/\mathrm{d}x$. However, since $\mathrm{d}\rho_0/\mathrm{d}x$ is only a function of x, the solution technique parallels that for the river induced flow. The solution to the density driven flow, which depth integrates to zero, is

$$\overline{u_{2\mathrm{d}}}(x, z) = \frac{1}{18}\gamma \frac{\mathrm{d}\rho_0}{\mathrm{d}x} d^3 \times [1 - 9z^2/d^2 - 8z^3/d^3]. \quad (18)$$

So the density driven flow is easily calculated, once the density structure in the estuary is determined. Previous analytical models (Jay, 1987; Jay and Smith, 1990b; and Officer, 1976) have found similar forms for $\overline{u_{2\mathrm{d}}}$ for use with a prescribed density field, but in general, the density structure in an estuary is coupled to the circulation and the effects of tidal mixing. Here lies the crux of this work: solving for the density structure in a well mixed estuary, given the tidal currents, the density at the mouth, and the river discharge. Once this density field is known, the gravitational circulation indeed follows from eq. (18). Then the residual currents in a tidally dominated, well mixed estuary can be determined from the linear combination of $\overline{u_{2\mathrm{nl}}}$, $\overline{u_{2\mathrm{r}}}$, and $\overline{u_{2\mathrm{d}}}$ and their relative strengths can be assessed.

To determine $\rho_0(x)$ and hence $\rho_0'(x)$, we will solve eqs. (11) and (14). Eq. (11) represents a balance at the fundamental frequency of the tidal forcing between the local rate of change of the tidal density fluctuation $\rho_1(x, z, t)$, the tidal advection of $\rho_0(x)$, and vertical mixing of the tidal density fluctuation. We will assume the tidal density fluctuation has the form

$$\rho_1(x, z, t) = \mathrm{Re}(\rho_0'(x)\, A'(x)\, \rho(z)\, \mathrm{e}^{it}). \quad (19)$$

Inserting this into eq. (11), we obtain a second order ordinary differential equation for $\rho(z)$,

$$\frac{\mathrm{d}^2\rho(z)}{\mathrm{d}z^2} - i\frac{2}{S_\mathrm{c}}\rho(z) = 2i\frac{U(z)}{S_\mathrm{c}},$$

with the boundary conditions $\mathrm{d}\rho/\mathrm{d}z|_0 = \mathrm{d}\rho/\mathrm{d}z|_{-d} = 0$.

Besides arbitrary Schmidt number, two special cases emerge: $S_\mathrm{c} = 0$ or $S_\mathrm{c} = 1$. If $S_\mathrm{c} = 0$, the local rate of change of ρ_1 is balanced only by the tidal advection of ρ_0. However, here the no buoyancy flux boundary condition at the bottom is violated. So this case is not allowed. Thus, some vertical diffusivity is required to avoid buoyancy flux through the bottom.

If $S_\mathrm{c} = 1$, the solution to $\rho(z)$ is

$$\rho(z) = \left(\frac{(1+i)\,d + \tanh(1+i)\,d}{2\sinh(1+i)\,d}\right)\cosh(1+i)\,z - 1 - \frac{(1+i)\,z\sinh(1+i)\,z}{2\cosh(1+i)\,d}. \quad (20)$$

For an arbitrary Schmidt number, the solution is

$$\rho(z) = \frac{1}{(S_\mathrm{c}-1)}\left[\frac{\sqrt{S_\mathrm{c}}\tanh(1+i)\,d}{\sinh((1+i)\,d/\sqrt{S_\mathrm{c}})} \times \cosh\left(\frac{(1+i)}{\sqrt{S_\mathrm{c}}}z\right) - \frac{\cosh(1+i)\,z}{\cosh(1+i)\,d}\right] - 1. \quad (21)$$

As $S_\mathrm{c} \to 1$, this solution agrees with eq. (20).

It remains to determine $\rho_0(x)$ from eq. (14). For the constant breadth estuary considered here, eq. (14) can easily be integrated once over x to obtain

$$-\frac{i}{2}|A'(x)|^2\,\rho_0'(x)\frac{1}{d}\int_{-d}^{0} U^*(z)\,\rho(z)\,\mathrm{d}z - R\rho_0(x) - K_x\rho_0'(x) = \text{const.}, \quad (22)$$

where u_1 and ρ_1 have been replaced by their functional forms, eqs. (16) and (19) respectively, const. is a constant, (*) represents the complex conjugate and $\rho(z)$ is given by either eq. (20) for $S_\mathrm{c} = 1$ or eq. (21) for arbitrary S_c. The integral is complex and thus can be expressed as

$$\int_{-d}^{0} U^*(z)\,\rho(z)\,\mathrm{d}z = \alpha + i\beta, \quad (23)$$

where α and β are given in M91 for both $S_\mathrm{c} = 1$ and for $S_\mathrm{c} \neq 1$. Thus, eq. (22) becomes

$$[(\beta - i\alpha)\,|A'(x)|^2 - 2dK_x]\,\rho_0'(x) - 2dR\rho_0(x) = \text{const.}_\mathrm{r} + i\,\text{const.}_\mathrm{i}, \quad (24)$$

where const. = const.$_r$ + i const.$_i$. Thus, for a given value of K_x, eq. (24) is a complex, ordinary first order differential equation for $\rho_0(x)$. Writing $\rho_0(x)$ as a complex quantity, $\rho_0(x) = \rho_{0_r}(x) + i\rho_{0_i}(x)$, eq. (24) can be expressed as two equations corresponding to real and imaginary parts.

The boundary conditions on the density field are now that, as $x \to \infty$, $\rho_{0_r}(x)$ and $\rho'_{0_r}(x)$ both must vanish. These conditions imply that a uniform pool of fresh water lies well upstream. Since $|A'(x)|^2$ vanishes as $x \to \infty$, it follows that const.$_r = 0$. Physically, this implies that there are no buoyancy sources or sinks within the estuary.

The solution to the density field can be obtained directly from eq. (24), where the constant on the right is a purely imaginary number. The homogeneous equation can be expressed as $\rho'_0(x) + P(x)\,\rho_0(x) = 0$, where

$$P(x) = \frac{2Rd}{(i\alpha - \beta)\,|A'(x)|^2 + 2K_x d}.$$

The solution is $\rho_0(x) = C/\mu(x)$, where C is a constant and $\mu(x)$ is the integrating factor, $\mu(x) = \exp(\int^x P(t)\,dt)$. This can easily be integrated (M91), and the complete solution to the inhomogeneous eq. (24) found as

$$\rho_0(x) = C \exp\left[-\frac{L_d}{2L_{dif}} \ln\left(1 + \frac{2K_x d \exp(2x/L_d)}{(i\alpha - \beta)(1/L_d^2 + 1/L_\lambda^2)} \right) \right] - i\frac{\text{const.}_i}{2Rd}, \tag{25}$$

where L_{dif} is defined to be the ratio K_x/R, a dimensionless diffusion length scale, L_λ a wavelength scale, and L_d a tidal dissipation length scale. L_λ and L_d are defined in Ianniello (1977a) and M91.

The boundary conditions now are applied to the real part of the density field: $\rho_{0_r}(x=0) = 1$ and $\rho'_{0_r}(x=0) = 0$ to determine the complex constant C. These imply that at the estuary mouth, we reach a pool of uniform ocean density. The final result for complex $\rho_0(x)$ is

$$\rho_0(x) = \left[\frac{(i\alpha - \beta)(1/L_d^2 + 1/L_\lambda^2) + 2K_x d}{(i\alpha - \beta)(1/L_d^2 + 1/L_\lambda^2) + 2K_x d \exp(2x/L_d)} \right]^{L_d/2L_{dif}} \times \left[1 + i\left(\frac{\beta}{\alpha} - \frac{2K_x d}{\alpha(1/L_d^2 + 1/L_\lambda^2)} \right) \right] - i\frac{\text{const.}_i}{2Rd}. \tag{26}$$

Thus, we have solved for the background density field in an infinite estuary of constant depth and breadth, given the tidal forcing at the mouth and the river discharge. However, there are two unknown parameters, N_z (which determines d, L_d, and L_λ) and K_x. Taking the derivative of eq. (26) completes the solutions to both the tidal density fluctuation eq. (19) and the density driven residual flow eq. (18).

In Fig. 2, the scaled density $\rho_{0_r}(x)$ is shown for the case when $\varepsilon = 0.1$, (weakly nonlinear), $d = 1$, $S_c = 1$, $R = 0.1$, and $L_d/L_{dif} = 2$. This results in a scaled value of 0.08 for K_x. When R is increased to order 1, so also is K_x increased. The abscissa is the channel length scaled by the tidal dissipation length scale, L_d. The mouth of the estuary (right in the figure) is at $x = 0$, and the positive x-direction is to the left. A scaled density of one indicates ocean water density, while a scaled density of zero represents fresh water density. Note the smooth transition from fresh to ocean density, with the maximum horizontal density gradient occurring near $x/L_d = 1$. This plot is representative of the scheme hypothesized by Hansen and Rattray (1965), with the central regime being almost linear with maximum gradient and with both ends tailing off gradually to terminal values in the river and ocean.

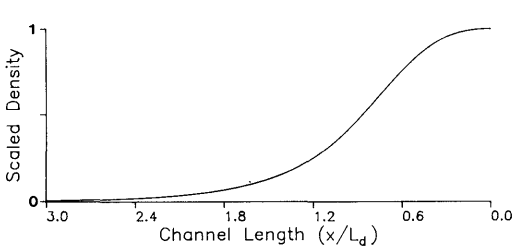

Fig. 2. Scaled density field $\rho_{0_r}(x)$ as a function of longitudinal position. At the mouth ($x = 0$), the scaled density is equal to one with zero slope, and the scaled density approaches zero upstream. Scaled parameters are: $d = 1$, $\varepsilon = 0.1$, $R = 0.1$, $S_c = 1$, and $L_d/L_{dif} = 2$.

The nature of the time averaged, vertically integrated buoyancy flux balance is best revealed

by plotting the terms in eq. (13) integrated once over x. For $b(x) = 1$ this is,

$$\frac{1}{d}\int_{-d}^{0} \overline{u_1 \rho_1}\, dz + \frac{1}{d}\int_{-d}^{0} \overline{u_2}\rho_0\, dz + \rho_0 \overline{u_1|_0 \eta_1} - K_x \rho_0'(x) = i\,\text{const.}_i. \quad (27)$$

The real part of each term, divided by R, is shown in Fig. 3. Positive values indicate a landward buoyancy transport, while negative values indicate a seaward buoyancy transport. The first term is the tidal buoyancy transport, and is denoted by the dashed line. The second and third terms represent the Eulerian subtidal buoyancy transport and the Stokes buoyancy transport, denoted by the solid and dashed-dotted lines, respectively. Both of these terms have been divided by 5 for plotting purposes. The Eulerian subtidal buoyancy transport everywhere exceeds the Stokes buoyancy transport and is of opposite sign. The sum of these is just the Lagrangian subtidal buoyancy transport. As represented here, the Lagrangian subtidal buoyancy transport is equal to the negative of the scaled density field shown in Fig. 2: -1 at the mouth and decaying to zero upstream. Thus, the Lagrangian subtidal buoyancy transport is of the same magnitude as the tidal and diffusive buoyancy transports. The latter term is represented by the dotted line. At the mouth, where $\rho_{0_r}'(x) = 0$, there is no diffusive buoyancy transport, so the balance is between the tidal buoyancy transport and the Lagrangian subtidal buoyancy transport. Progressing landward far from the mouth, the tidal buoyancy transport contribution diminishes, due to bottom friction retarding the tidal advance. There, diffusive buoyancy transport is required to balance the Lagrangian subtidal buoyancy transport.

As the parameter K_x is diminished, the solution to $\rho_{0_r}(x)$ upstream becomes negative, a physically meaningless result, see Fig. 4a. Without horizontal

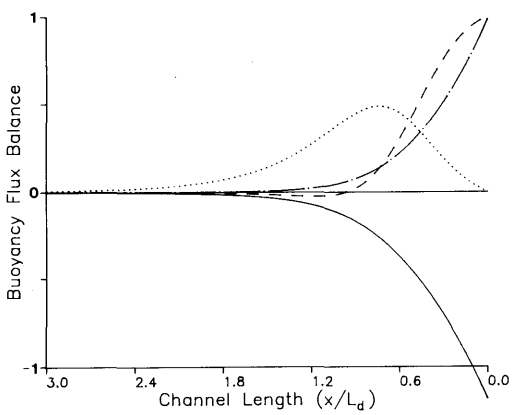

Fig. 3. Buoyancy flux balance expressed in eq. (27) as a function of longitudinal position. Positive values indicate a landward buoyancy transport, while negative values indicate seaward buoyancy transport. The tidal buoyancy transport (dashed line) is landward at the mouth and decays upstream. Both the Eulerian subtidal buoyancy transport (solid line) and the Stokes buoyancy transport (dashed-dotted line) have been divided by 5 for plotting purposes. Their sum is just the Lagrangian subtidal buoyancy transport; here -1 at the mouth and decaying to zero upstream. The diffusive buoyancy transport (dotted line) is positive and is necessary to balance the seaward Lagrangian buoyancy transport upstream.

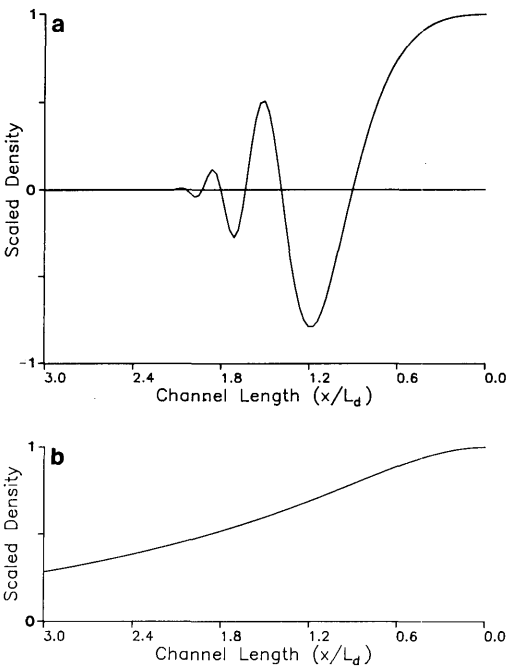

Fig. 4. (a) Same as Fig. 2 but now without horizontal diffusion, K_x. The solution, expressed in eq. (28), contains an oscillatory part that causes the scaled density field to become negative; a physically meaningless result. (b) Same as Fig. 2 but now $L_d/L_{dif} = 0.5$. Here the horizontal diffusivity has been increased such that at 3 dissipation length scales away from the mouth, the scaled density is about 0.3. The solution for large K_x approaches $\rho_{0_r}(x) = 1$ for any finite x.

diffusion ($K_x = 0$), the balance expressed in eq. (24) is between the tidal buoyancy transport and the Lagrangian subtidal buoyancy transport. The solution for $\rho_{0_r}(x)$ then is (M91)

$$\rho_{0_r}(x) = \exp\left[-\frac{\beta R d L_d}{(\alpha^2+\beta^2)(1/L_d^2 + 1/L_\lambda^2)} \times (1 - \exp(2x/L_d)) \right] \times \left\{ \cos\left[-\frac{\alpha R d L_d}{(\alpha^2+\beta^2)(1/L_d^2 + 1/L_\lambda^2)} \times (1 - \exp(2x/L_d)) \right] - \frac{\beta}{\alpha} \sin\left[-\frac{\alpha R d L_d}{(\alpha^2+\beta^2)(1/L_d^2 + 1/L_\lambda^2)} \times (1 - \exp(2x/L_d)) \right] \right\}. \quad (28)$$

Notice that this solution has an exponentially decaying part and an oscillatory part. It is the latter that causes the solution to have negative values for the scaled density field which are physically meaningless. As $K_x \to 0$, the solution represented in eq. (26) approaches the solution in eq. (28). Therefore, a minimum horizontal diffusivity is required if the scaled density field is to be non-negative.

As K_x is increased, the diffusive buoyancy transport in eq. (27) becomes dominant, resulting in a longer length to reach a scaled density near zero, see Fig. 4b. The limiting case of large K_x is an estuary with uniform density equal to the density at the mouth, $\rho_{0_r}(x) = 1$, for any finite x. Thus the model results show that there is a narrow range of values for K_x that correspond to physically meaningful results.

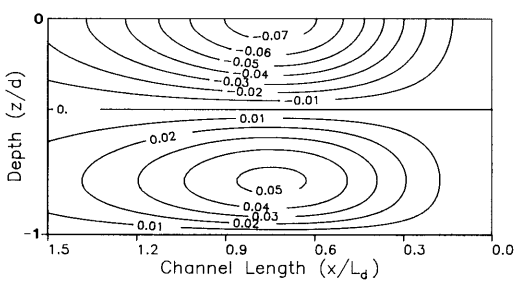

Fig. 5. Scaled density driven residual flow for the same parameters used in Fig. 2 ($\varepsilon = 0.1$, $d = 1$, $S_c = 1$, $L_d/L_{dif} = 2$, and $R = 0.1$). Surface flow is seaward and bottom flow is landward with a constant level of no motion.

Now we can discuss the scaling chosen for K_x in Section 2. Physically, the buoyancy balance in an estuary landward of the region of strong tidal transport is maintained by the downstream advection of buoyancy by the Lagrangian subtidal flow against the upstream transport by diffusion. To obtain this balance, the scaling for K_x must not exceed the scale for the residual flow, $\varepsilon^2 c$, multiplied by the longitudinal length scale, c/σ. Thus,

$$K_x \leqslant O\left(\varepsilon^2 c \frac{c}{\sigma}\right) = O\left(\frac{\varepsilon^2 c^2}{\sigma}\right),$$

consistent with the choice in Section 2.

The dimensional value for the horizontal diffusion coefficient is approximately 600 $m^2 s^{-1}$ for the choice of parameters corresponding to Fig. 3. This value is consistent with the range of values cited in the literature for K_x. Bowden (1963) gives a range of values for horizontal diffusivity of 160–360 $m^2 s^{-1}$ for the Mersey, Hansen (1967) used a value of 200 $m^2 s^{-1}$ for the Narrows of the Mersey, Paulson (1969) determined a value of 100 $m^2 s^{-1}$ for the Delaware Estuary for a low flow discharge of 56.6 $m^3 s^{-1}$ at Trenton, Thatcher and Harleman (1972) computed values of K_x for the Delaware Estuary between 500–1500 $m^2 s^{-1}$, and Oey (1984) computed a value of 500 $m^2 s^{-1}$ for the Hudson during high river flow.

The corresponding scaled gravitational circulation, $\overline{u_{2d}}$, for $\varepsilon = 0.1$, $d = 1$, $S_c = 1$, $R = 0.1$, and $L_d/L_{dif} = 2$, is illustrated in Fig. 5. The surface water flows seaward, while at depth the flow is landward. The maximum flow is positioned at the maximum horizontal density gradient. At the mouth, where we imposed $\rho'_{0_r}(x=0) = 0$, the density driven flow is zero since here there is no forcing. Increasing R increases $\overline{u_{2r}}$ and to a lesser extent $\overline{u_{2d}}$, while decreasing the nonlinearity of the system results in an increase in γ, which then strengthens the density driven flow relative to the tidal flow.

The total residual Eulerian flow, $\overline{u_{2nl}} + \overline{u_{2d}} + \overline{u_{2r}}$, for the case shown in Fig. 5, is shown in Fig. 6a. Notice that the flow is seaward at all depths, indicating the nonlinearly induced and river flows

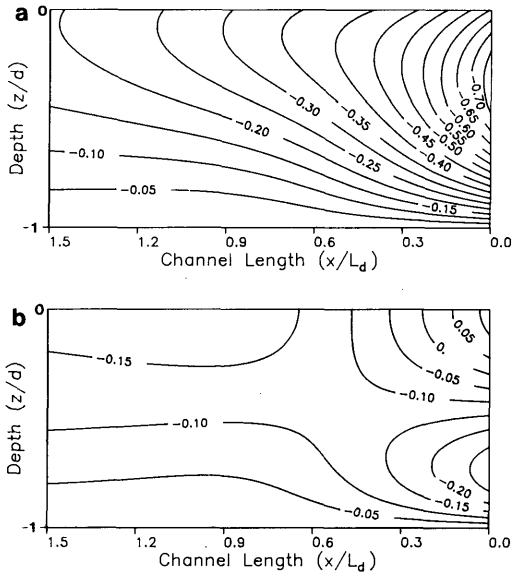

Fig. 6. (a)Total residual Eulerian flow, $\overline{u_{2nl}}+\overline{u_{2d}}+\overline{u_{2r}}$, for the parameters used in Fig. 5. (b) Total residual Lagrangian flow, $\overline{u_{2l}}+\overline{u_{2d}}+\overline{u_{2r}}$, for the parameters used in Fig. 5.

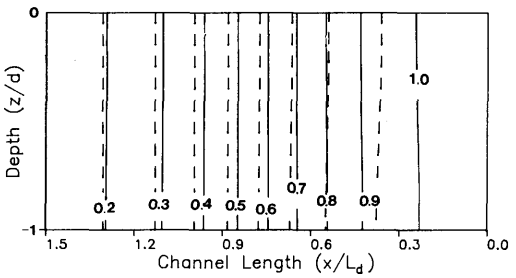

Fig. 7. The scaled density field, $\rho_{0_r}(x)+\varepsilon\rho_1(x, z, t)$ for two stages of the tidal cycle, flood tide (solid line) and ebb tide (dashed line).

dominate the density driven flow. The Lagrangian residual flow is shown in Fig. 6b. Here the nonlinearly induced Lagrangian residual flow, $\overline{u_{2l}}$, is added to both the density driven and river induced flows. These latter two residual flows do not contain a Stokes drift, and so the Lagrangian and Eulerian flows are identical. At the surface near the mouth, we observe weak landward flow, resulting from the strong Stokes drift (calculated from the nonlinearly induced residual flow) and the lack of the gravitational flow here (since at the mouth, $\rho_0'(x=0)=0$); otherwise the flow is seaward.

To unscale the above velocity plots the values are multiplied by $\varepsilon^2 c$. When $\varepsilon=0.1$ and the depth is 10 m, a scaled velocity of 0.1 is equal to a dimensional flow of approximately 1 cm s^{-1}.

Finally, we can investigate the tidal density fluctuation field for different stages of the tidal cycle. (Scaled time $t=0$ corresponds to high water at the mouth.) During the flood stages of the tidal flow, the density fluctuation field is unstable, heavy water overlaying light water. This results from the stronger tidal currents near the surface than at depth bringing into the estuary denser ocean water. In nature this process will enhance the vertical mixing and so help maintain the well mixed density structure. During the ebb tidal cycle, denser water is transported seaward at the surface farther than at depth. This condition is stably stratified. The scaled density field, $\rho_{0_r}(x)+\varepsilon\rho_1(x, z, t)$ for the flood and ebb stages of the tidal cycle are shown in Fig. 7. During the flood stage, the isopycnals (denoted by the solid lines) are compressed near the mouth, while during the ebb tidal cycle, the isopycnals (represented by the dashed lines) are spread apart. However, throughout the complete tidal cycle, the vertical density gradient is quite small, consistent with the well mixed condition assumed.

4. The reflecting wall solution

This section parallels the preceding section, but now the estuary has finite length, L, and variable breadth, $b(x)$. These constraints change the first order tidal solution, but the scaled tidal governing equations remain the same. Now we impose the boundary condition that the tidal flow is zero at the wall, $u_1(x=L)=0$ which implies $A'(x=L)=0$. The functional form for $A(x)$ is now (for an exponentially decaying scaled breadth defind as $b(x)\equiv\exp(-\kappa x)$, where κ is the exponential decay factor)

$$A(x)=(1-F)\exp(r_1 x)+F\exp(r_2 x), \qquad (29)$$

where

$$r_1=[\kappa+(\kappa^2-4/D)^{1/2}]/2,$$

$$r_2=[\kappa-(\kappa^2-4/D)^{1/2}]/2,$$

$$F=(r_1\exp(r_1 L))/[r_1\exp(r_1 L)-r_2\exp(r_2 L)].$$

To complete the first order tidal solution, the vertical velocity w_1 can be found from vertically integrating the continuity equation (2). See Ianniello (1977a) and M91 for details of the tidal solution.

Since the mathematical problem is still linear in the forcing terms, we can separate the three sources of residual flow as in Section 3. Since the tidal solution has been altered by the introduction of the reflecting wall at a distance L from the mouth and since the breadth is no longer constant, the rectified tidal flow has also changed. The solution appears in Ianniello (1977a, 1979) and in M91. Because the breadth is allowed to vary, the continuity equation for the river induced flow is

$$b(x)\frac{1}{d}\int_{-d}^{0}\overline{u_{2r}}\,dz = -R. \tag{30}$$

The solution to the river induced flow,

$$\overline{u_{2r}}(x,z) = \frac{3R}{2b(x)\,d^2}(z^2-d^2), \tag{31}$$

is now a function of longitudinal position, since the breadth is no longer constant. The strongest flow is at the head, where the estuary is narrowest, and decays toward the mouth.

The form of solution to the density driven flow is identical, see eq. (18), but the density field has changed. To determine $d\rho_0/dx$ for the finite length, variable breadth estuary, we will again solve eqs. (11) and (14) by assuming that ρ_1 can be expressed in the form of eq. (19). Substituting eqs. (16), (19), and (23) (since the vertical distributions $U(z)$ and $\rho(z)$ are identical) into eq. (14) we obtain

$$\rho_0''(x)[b(x)(\beta-i\alpha)\,|A'(x)|^2 - 2db(x)\,K_x] + \rho_0'(x)\left[(\beta-i\alpha)\frac{d}{dx}(b(x)\,|A'(x)|^2) - 2dR\right] = 0. \tag{32}$$

This equation reduces to eq. (24) if $b(x)=1$. Eq. (32) can be expressed as $\rho_0''(x)+P(x)\rho_0'(x) = 0$, where $P(x)$ is complex. Thus $P(x) = P_r(x)+iP_i(x)$ where $P_r(x)$ and $P_i(x)$ are given in M91.

Since $\rho_0(x)$ is again complex, eq. (32) can be written as two equations corresponding to real and imaginary parts. Solving for $\rho_{0_i}'(x)$ from the real equation, taking its derivative, and substituting into the imaginary equation, we obtain a third order equation for $\rho_{0_r}(x)$,

$$P_i(x)\,\rho_{0_r}'''(x) + \rho_{0_r}''(x)[2P_r(x)\,P_i(x) - P_i'(x)] + \rho_{0_r}'(x)[P_r'(x)\,P_i(x) - P_r(x)\,P_i'(x) + P_r^2(x)\,P_i(x) + P_i^3(x)] = 0. \tag{33}$$

This equation can be solved for $\rho_{0_r}(x)$ subject to three boundary conditions. Here again, $\rho_{0_r}(x=0) = 1$, and $\rho_{0_r}'(x=0)=0$, as before. For insight into the remaining boundary condition, we investigate the behavior of the solution in the preceding section far upstream.

From the constant breadth estuary in Section 3, as $x\to\infty$ both $\rho_{0_r}(x)$ and $\rho_{0_r}'(x)$ approach zero. Therefore, the real part of the constant of integration was zero (const.$_r$ $=0$ in eq. (24)). For x sufficiently large such that the tidal buoyancy flux contribution can be omitted, the buoyancy balance is maintained by diffusive transport against Lagrangian subtidal transport. This suggests that for the variable breadth estuary the appropriate condition at the wall (where there is no tidal buoyancy transport) is simply

$$\rho_{0_r}'(L) = -\frac{R}{K_x}\rho_{0_r}(L). \tag{34}$$

Before adopting this for the variable breadth case, however, we must investigate the form of solution near the wall.

At the wall ($x=L$), $P_i(L)=0$ (see M91, since both $|A'(L)|^2$ and $d\,|A'(x)|^2/dx|_{x=L}$ equal zero). Therefore, to obtain the solution behavior near the wall, the method of Frobenius is used with a change of coordinates. Letting $\xi = L-x$ and $\phi(\xi) = \rho_{0_r}(x) = \sum_{n=0}^{\infty} C_n\xi^{n+p}$, and expanding eq. (33) for small ξ, it can be shown that the roots of the indicial equation are $p=3$, $p=1$, and $p=0$. There are no repeated roots, and the distinct roots differ by integers. Thus the solution near the wall (the "inner" solution) is found to be the power series

$$\phi(\xi) = C_0 + C_1\left(\xi + \frac{R}{2b_h K_x}\xi^2\right) + C_2\left(\xi^3 + \left(\frac{\kappa}{4}+\frac{R}{b_h K_x}\right)\xi^4 + \cdots\right),$$

where $b_h = e^{-\kappa L}$. Note that the first appearance of κ, i.e., the effect of variable breadth, does not occur until $O(\xi^4)$. Therefore, for small ξ, the upstream boundary condition is unaltered by breadth variations.

This invariance can also be seen from an x-integrated form of eq. (13),

$$d^{-1}b(x)\int_{-d}^{0}\overline{u_1\rho_1}\,dz + d^{-1}b(x)\int_{-d}^{0}\overline{u_2\rho_0}\,dz + b(x)(\overline{u_1\rho_0})|_{z=0}\eta_1 - b(x)\,K_x\rho_{0_r}'(x) - \kappa K_x\int_x^L b(x)\,\rho_{0_r}'(x)\,dx = 0, \quad (35)$$

where the last two terms on the left hand side of eq. (35) result from an integration by parts of $-b(x)\,K_x\,d^2\rho_0/dx^2$. If $\kappa = 0$, then $b(x) = 1$, and eq. (35) becomes identical to eq. (27). But now note that as $x \to L$, the last term on the left in eq. (35) vanishes. Thus near the wall, the effect of breadth variations diminishes. Therefore, regardless of the estuary configuration, the upstream boundary condition is just eq. (34).

Applying this condition to the "inner" solution, we find that $C_1 = (R/b_h K_x)\,C_0$. The resulting solution near the wall then becomes

$$\rho_{0_r}(x) = C_0\left\{1 + \frac{R}{b_h K_x}(L-x) + \frac{1}{2}\left(\frac{R}{b_h K_x}(L-x)\right)^2\right\} + C_2\left\{(L-x)^3 + \left(\frac{\kappa}{4} + \frac{R}{b_h K_x}\right)(L-x)^4 + \cdots\right\}. \quad (36)$$

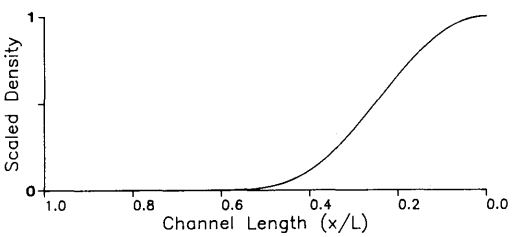

Fig. 8. Scaled density field $\rho_{0_r}(x)$ as a function of longitudinal position. Here, the channel length is $L/L_d = 3$, and $\kappa = 1$. Other parameters are consistent with the straight channel case ($d = 1$, $\varepsilon = 0.1$, $R = 0.1$, and $S_c = 1$) but now $L_d/L_{dif} = 0.5$.

Equation (33) can now be solved using a numerical routine away from the wall using the three boundary conditions, and matched to the "inner" solution at a particular point near the wall to determine C_0 and C_2. This completes the formal solution to the density field for a finite length estuary of variable breadth, given the river discharge and the tidal forcing.

Fig. 8 shows the density field for an estuary of length $L/L_d = 3$, or a nondimensional estuary length $L = 3.8$, when $\varepsilon = 0.1$, $L_d/L_{dif} = 0.5$, $d = 1$, $S_c = 1$, $\kappa = 1$ and $R = 0.1$. More horizontal diffusion is required when the estuary narrows, so $L_d/L_{dif} = 0.5$ now, whereas $L_d/L_{dif} = 2$ for the straight estuary. Again we notice the smooth transition from fresh water to ocean water, but now

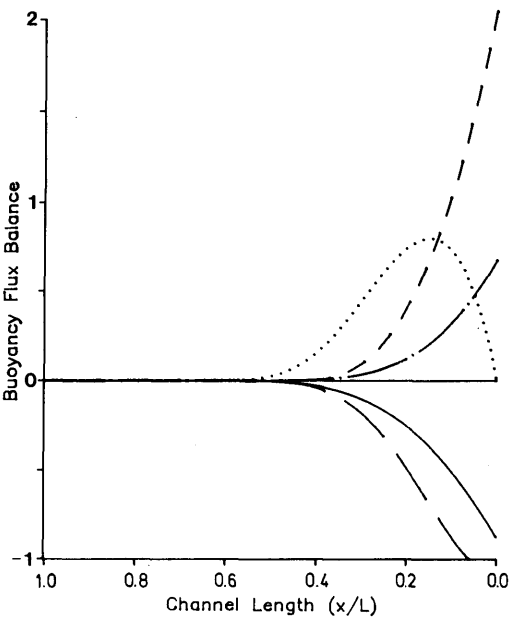

Fig. 9. Buoyancy flux balance expressed in eq. (35) as a function of longitudinal position for the case shown in Fig. 8. The tidal buoyancy transport (dashed line) is landward (positive) at the mouth and balances the Lagrangian buoyancy transport expressed as the sum of the Eulerian buoyancy transport (solid line) and the Stokes buoyancy transport (dashed-dotted line), each scaled by 5 for plotting purposes. The diffusive buoyancy transport (dotted line) is landward and balances the Lagrangian buoyancy transport upstream when the tidal buoyancy transport vanishes. The variable breadth diffusive buoyancy transport (large dashed line) is negative to balance the strengthened tidal landward buoyancy transport due to the funnel shape of the channel.

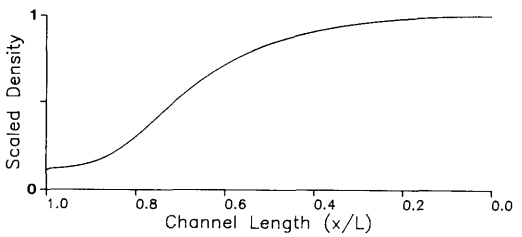

Fig. 10. Same as Fig. 8 but now for a shortened channel, $L/L_d = 1$. Note that a scaled density of zero at the head is not obtained. Here, $R = 0.1$ and $L_d/L_{dif} = 1.5$.

the maximum gradient occurs near $x/L = 0.3$. By comparing this figure to Fig. 2 where $\kappa = 0$, we see that the effect of varying breadth is to shorten the longitudinal scale of the salt intrusion in the estuary. This is due to the increased river flow near the head where the estuary is narrowest. Fig. 9 illustrates the 5 term balance expressed in eq. (35). The small dashed line represents the tidal buoyancy transport, the dotted line the diffusive buoyancy transport, and the solid and dashed-dotted lines the Eulerian and Stokes residual buoyancy transports, respectively, divided by 5 for plotting purposes. The new term in eq. (35), $-\kappa K_x \int_x^L b(x)\, \rho'_{0_t}(x)\, dx$, denoted by the long dashed line in Fig. 9, is the variable breadth diffusive buoyancy flux term and is negative, indicating a seaward buoyancy transport. This term is required to offset the increased tidal landward buoyancy transport created by the narrowing of the estuary. As $\kappa \to 0$ and $x \to L$, this term vanishes.

For the remaining figures, the exponential decay factor will be equal to one, and the estuary length will be one tidal dissipation length scale ($\kappa = 1$, and $L/L_d = 1$). Fig. 10 shows the scaled lowest order density field for the case when $\varepsilon = 0.1$, $L_d/L_{dif} = 1.5$, and $R = 0.1$. Note that the density field does not reach a value of zero (fresh water), since the estuary is too short. Fig. 11 shows the scaled density driven circulation resulting from the density distribution in Fig. 10. Near the mouth, the horizontal density gradient is slight, so the density driven flow there is weak. The maximum flow is positioned at the place of maximum horizontal density gradient (near $x/L = 3/4$), and is seaward near the surface and landward at depth. Decreasing to $\varepsilon = 0.05$ effectively increases the relative strength of the density driven flow. The complete Eulerian and Lagrangian estuarine subtidal flows for $\varepsilon = 0.1$ are illustrated in Figs. 12a, b, respectively. Here again, the landward bottom flow of the gravitational circulation is masked by the dominance of the river and rectified tidal seaward flows. When the measure of the nonlinearity of the system is decreased by a factor of two to $\varepsilon = 0.05$ (not shown), the landward bottom flow driven by the density gradient dominates.

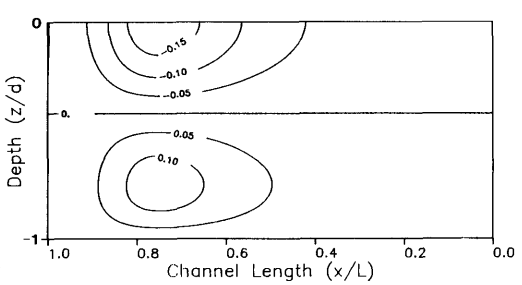

Fig. 11. Scaled density driven residual flow for the density field shown in Fig. 10.

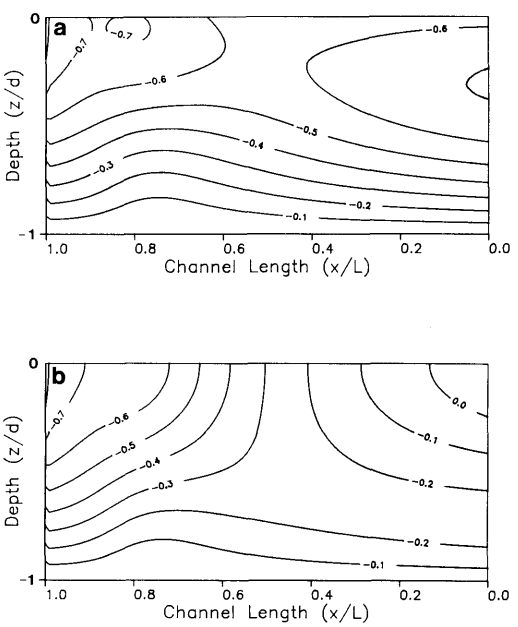

Fig. 12. (a) Total residual Eulerian flow, $\overline{u_{2nl}} + \overline{u_{2d}} + \overline{u_{2r}}$, for the parameters used in Fig. 10. (b) Total residual Lagrangian flow, $\overline{u_{2l}} + \overline{u_{2d}} + \overline{u_{2r}}$, for the parameters used in Fig. 10.

5. Conclusions

Here we've described an analytical, two-dimensional model of residual flows in tidally dominated, well-mixed estuaries. The residual flows originate from tidal rectification, river discharge, and density differences within the estuary. The model framework is an extension of the work of Ianniello (1977a, 1977b, 1979, and 1981) with the addition of the baroclinic pressure gradient force in the longitudinal momentum equation. The dependent variables are expanded in asymptotic series in powers of $\varepsilon \equiv \eta_m/h$, the tidal surface elevation at the mouth divided by the mean depth. This parameter measures the strength of the nonlinear advection terms in the governing equations. As long as this ratio is small, the estuary is only weakly nonlinear and the series expansion is valid.

Because the estuaries treated are tidally dominated, the strength of the baroclinic pressure gradient can be no larger than order ε. This excludes the baroclinic tides that are present in highly stratified estuaries. The degree of vertical stratification is restricted to be order ε or less.

The crux of this work centered around finding the lowest order density field, given the tidal forcing and density at the mouth, and river discharge upstream. Two free parameters of the model are the vertical eddy viscosity, contained in the scaled depth d, and the horizontal diffusion coefficient K_x determined from the ratio of L_d/L_{dif}. However from scaling arguments, the appropriate range of values for K_x is limited. In particular, there exists a lower bound on K_x such that the scaled density field is non-negative upstream. The inherently nonlinear problem allowed analytical solutions, provided the density field was well mixed vertically to lowest order. By using the continuity equation, the problem could be reformulated as a linear one.

Analytical solutions were obtained in Section 3 for the ideal case of an infinite length estuary of constant depth and breadth. The tidal wave was damped by bottom friction, and the longitudinal distance was scaled by the tidal dissipation length, L_d. Within a few L_d, the density reached that of freshwater. The major buoyancy balance at the mouth was between the landward tidal buoyancy transport against the seaward Lagrangian buoyancy transport. Further upstream where the tidal buoyancy transport is reduced, the horizontal diffusive buoyancy transport balances the Lagrangian buoyancy transport. Formal solutions found for zero horizontal diffusion showed a scaled density field that oscillated between positive and negative values, clearly a physically meaningless result. Thus, the tidal diffusion of buoyancy was not enough to obtain a balance upstream. The model tells us that we need an explicit K_x, here assumed constant, to balance the seaward net Lagrangian buoyancy transport upstream. K_x accounts for many other dispersive processes other than tidal diffusion, including shear flow dispersion and lateral diffusion. Typical lower bound values for diffusion were in the range of those inferred in published analyses of observations.

Section 4 treated an estuary with a tidal barrier or head at a finite length and variable breadth that decreased exponentially towards the head. The buoyancy balance was the same, but with an additional horizontal diffusive transport due to the varying breadth. The governing equation for the scaled density field became third order, so three boundary conditions were needed. At the wall, a solution was found using the method of Frobenius, and was matched to a numerical solution away from the wall.

The major result of this work was the discovery of how the density field is coupled to the circulation in tidally dominated, well-mixed estuaries. Through the use of the continuity equation, it was found that the buoyancy balance in the estuary is between three processes: tidal buoyancy transport, Lagrangian subtidal buoyancy transport, and horizontal diffusive buoyancy transport. The density field, given the tidal forcing and the river discharge, was then calculated from this balance. The resulting density distribution was then used to determine the density driven residual flow. Thus, it was not required that the density field be prescribed, as in some earlier analytical models, in order to calculate the density driven residual flow.

6. Acknowledgements

This work is part of my PhD dissertation prepared under the guidance of Richard Garvine. I am grateful for his advice and financial support of this work through Grant OCE-8711299 from the National Science Foundation.

REFERENCES

Bowden, K. F. 1963. The mixing processes in a tidal estuary. *Internat. J. Air and Water Pollution 7*, 343–356.

Chatwin, P. C. 1976. Some remarks on the maintenance of the salinity distribution in estuaries. *Estuarine and Coastal Mar. Sci. 4*, 555–566.

Feng, S., Cheng, R. T. and Xi, P. 1986. On tide-induced Lagrangian residual current and residual transport 2. Residual transport with application in South San Francisco Bay, California. *Water Resour. Res. 22*, 1635–1646.

Hansen, D. V. 1967. Salt balance and circulation in partially mixed estuaries. In: *Estuaries*, Publication No. 83, American Association for the Advancement of Science, Washington, DC, 45–51.

Hansen, D. V. and Rattray, M. Jr. 1965. Gravitational circulation in straits and estuaries. *J. Mar. Res. 23*, 104–122.

Hansen, D. V. and Rattray, M. Jr. 1966. New dimensions in estuary classification. *Limnol. Oceanogr. 11*, 319–326.

Ianniello, J. P. 1977a. *Non-linearly induced residual currents in tidally dominated estuaries.* PhD dissertation, University of Connecticut, USA, 300 pp.

Ianniello, J. P. 1977b. Tidally induced residual currents in estuaries of constant breadth and depth. *J. Mar. Res. 35*, 755–786.

Ianniello, J. P. 1979. Tidally induced residual currents in estuaries of variable breadth and depth. *J. Phys. Oceanogr. 9*, 962–974.

Ianniello, J. P. 1981. Comments on tidally induced residual currents in estuaries: Dynamics and near-bottom flow characteristics. *J. Phys. Oceanogr. 11*, 126–134.

Jay, D. A. 1987. *Residual circulation in shallow, stratified estuaries.* PhD dissertation, University of Washington, USA, 173 pp.

Jay, D. A. and Smith, J. D. 1990a. Residual circulation in shallow estuaries. 1. Highly stratified, narrow estuaries. *J. Geophys. Res. 95*, 711–731.

Jay, D. A. and Smith, J. D. 1990b. Residual circulation in shallow estuaries. 2. Weakly stratified and partially mixed, narrow estuaries. *J. Geophys. Res. 95*, 733–748.

Longuet-Higgins, M. S. 1969. On the transport of mass by time varying ocean currents. *Deep Sea Res. 16*, 431–447.

McCarthy, R. K. 1991. *A two-dimensional analytical model of density-driven residual currents in tidally dominated, well-mixed estuaries.* PhD dissertation, University of Delaware, USA, 174 pp.

Oey, L.-Y. 1984. On steady salinity distribution and circulation in partially mixed and well mixed estuaries. *J. Phys. Oceanogr. 14*, 629–645.

Officer, C. B. 1976. *Physical oceanography of estuaries (and associated coastal water).* John Wiley and Sons, New York, 465 pp.

Paulson, C. G. 1969. The longitudinal diffusion coefficient in the Delaware River estuary as determined from a steady-state model. *Water Resources Research 5*, 59–67.

Pritchard, D. W. 1952. Salinity distribution and circulation in the Chesapeake Bay estuarine system. *J. Mar. Res. 11*, 106–123.

Pritchard, D. W. 1954. A study of the salt balance in a coastal plain estuary. *J. Mar. Res. 13*, 133–144.

Pritchard, D. W. 1956. The dynamic structure of a coastal plain estuary. *J. Mar. Res. 15*, 33–42.

Rattray, M. Jr. and Hansen, D. V. 1962. A similarity solution for circulation in an estuary. *J. Mar. Res. 20*, 121–133.

Thatcher, M. L. and Harleman, D. R. F. 1972. *A mathematical model for the prediction of unsteady salinity intrusion in estuaries.* R. M. Parsons Lab. Rep. 44, MIT.

Printed in Belgium